EXAFS Data Analysis of Vitamin B_{12} Model Compounds − A Methodological Study

Emiliano Fonda,[a,b,c] Alain Michalowicz,[c] Lucio Randaccio,*[a] Giovanni Tauzher,[a] and Gilberto Vlaic[a,b,d]

Keywords: EXAFS spectroscopy / Cobaloxime / Vitamins

In view of several controversial EXAFS results on cobalamins and B_{12} model compounds published in the last ten years, a methodological study is presented to explain the origin of these controversial results and to propose how to improve EXAFS structural-parameter refinement. The advantages and limitations of first-shell filtering, constrained refinement, and the importance of the mapping technique are described in order to suggest and encourage improvement of data-analysis codes. The conclusions can be generalized and applied to the EXAFS analysis of the majority of metal complexes

Introduction

The B_{12}-based enzymes are among the few cofactors known so far that contain a metal−carbon bond. These coenzymes belong to the alkylcobalamin series (RCbl). They consist of a cobalt corrinoid with a pendant nucleotide, which occupies five coordination sites of a pseudo-octahedral Co^{III}, the sixth position being occupied by an R alkyl group or by a CN ligand in vitamin B_{12} itself (Scheme 1).[1,2] All the currently known B_{12} enzymatic reactions involve the making and breaking of the Co−C bond. In order to better understand the structure and reactivity of cobalamins, simple models have been proposed and investigated. The cobaloximes $LCo(DH)_2R$ (L = Lewis base, $(DH)_2$ = bis(dimethylglioximate)] represent the most widely studied class of models.[3] Such model studies have complemented those on cobalamins well,[1,2] thereby providing clues into the elusive mechanisms of B_{12}-dependent enzymatic processes, particularly those involving the homolytic Co−C cleavage.[3] One of the problems was the knowledge of the accurate structure of cobalamins. Up to a few years ago, for reasons previously reported,[4] the available structural determinations, based on conventional X-ray sources, were of poor accuracy, in contrast with the very accurate structures of the simple models.[3] Only recently[4,5,6] have the first accurate determinations based on synchrotron diffraction data appeared.

However, the interest in the structure of these systems has also prompted several Extended X-ray Absorption Fine Structure (EXAFS) studies, principally on cobalamins,[7,8,9] but also on models[10] and more recently on the B_{12} coenzyme bound in methylmalonyl-coenzyme A mutase.[11,12]

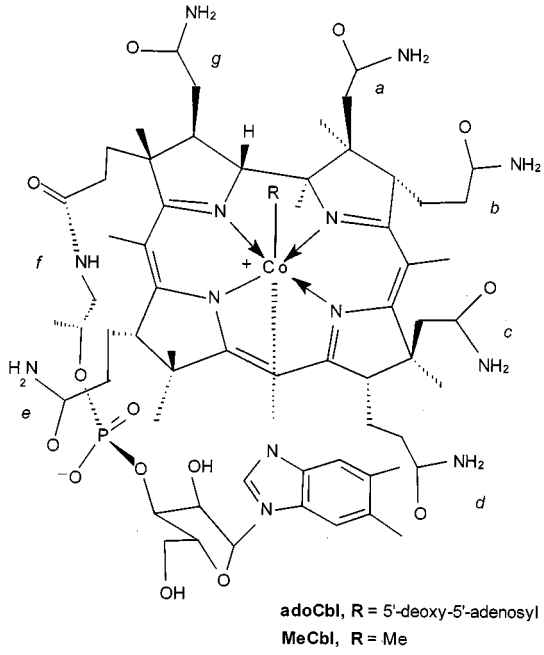

Scheme 1

The main advantage of EXAFS with respect to X-ray Diffraction (XRD) is that it does not require crystalline samples and can be used in solution. Although EXAFS is expected to be an order of magnitude less accurate than XRD for small molecules,[13] EXAFS can be exploited in the structural studies of metallo-proteins when XRD is not available and, more importantly, to follow the variations in the coordination about the metal centres within the active site.[14] In recent years, as the number of EXAFS results on B_{12} derivatives[7,8,9] and related model compounds[10] has increased, the discussion of these results, when compared to crystal structures, has become controversial.

In almost all EXAFS works, the Co−ligand distances have been deduced from fits of the first shell Fourier-filtered spectrum. This method, largely used since the pioneering

[a] Dip. Scienze Chimiche, Università degli Studi di Trieste, Via Licio Giorgieri 1, 34127 Trieste, Italia
[b] Sincrotrone Trieste SCpA, SS14 km 163.5, 34012 Basovizza (Trieste), Italia
[c] Laboratoire GPMD, Univ. Paris XII-Val de Marne, 61, Avenue du Général de Gaulle, 94010 Créteil Cedex, France
[d] INFM, Laboratorio TASC, Padriciano 99, 34012 Trieste, Italia

  1434−1948/01/0505−1269 $ 17.50+.50/0

works in EXAFS,[15] has been criticized[16,17] in the case of B_{12} for two reasons: i) Fourier filtering may lose a part of the actual signal. In fact, the contribution of the axial ligands from between the first and second coordination spheres may overlap; ii) The information contained in the first shell Fourier-filtered signal is insufficient to allow for any reliable determinations of the coordination distances of the equatorial Co−N distances and of the two axial ligands. For instance, Chance used this method to determine the local structure of Co in cobalamins and enzyme-bound cobalamins.[7−9] However, in the case of $(H_2OCbl)[ClO_4]$, there were dramatic discrepancies between the accurate XRD structure and that obtained by EXAFS.[8] In fact, the EXAFS value of the Co−N axial distances in H_2OCbl^+ [2.14(3) Å] and in $Co^{II}Cbl$ [1.99(3) Å] appear to be reversed with respect to those determined by XRD [1.925(2) and 2.13(2) Å, respectively]. Furthermore, the *trans* influence of H_2O, CN and SO_3-Cbl appeared to be very similar from EXAFS analysis, the *trans* axial Co−N distances varying in the range 2.14(3)−2.16(4) Å.[9] On the contrary, XRD results indicate a dramatic lengthening of the axial Co−N bond in SO_3^{2-} [2.149(5) Å][5a] and CN^- [2.041(3) Å] derivatives,[5b] with respect to the value of 1.925(2) Å found in the aqua derivative.[6]

Recently, more reliable methods than Fourier filtering of the first shell were employed. Giorgetti et al.[10] worked on a series of Costa-type models $(H_2O)Co(DO)(DOH)R$, in which R = CH_2CF_3, CH_2CO_2Me Me, CH_2Ph, *i*Pr, and (DO)(DOH)=*N*,*N*′-propanediylbis(2,3-butanedione-2-imine-3-oxime). These authors studied the variation of the distances between cobalt and its first neighbours, while the rest of the structure was kept constant. Multiple-scattering (MS) calculations and unfiltered data had been employed. Nevertheless, analogous large discrepancies (0.15−0.2 Å) in the axial coordination bond lengths, also including opposite trends of the R *trans* influence, were detected in a subsequent XRD study.[18] Scheuring et al.[11] employed the so-called "global-mapping technique" to study B_{12} in the glutamate mutase enzyme. Unfiltered data sets and MS calculations were employed. This technique consists of mapping the value of the χ^2 versus the variation of the distances of two ligands, while the rest of the structure is kept fixed. The minima in the map correspond to possible distances. Two possible Co−N axial distances were found. Between the short (2.17 Å) and the long (2.6 Å) distances, they chose the latter, because an XRD structure[19] of the B_{12}-enzyme indicated a long distance. Champloy et al.[12] worked on methylcobalamin bound to the enzymes, glutamate mutase and 2-methylene glutarate mutase. They found identical EXAFS spectra for the free and enzyme-bound MeCbl and two minima at the same distances as those of Scheuring et al.[11] In the free Me-Cbl, the Co−N axial distance is "short" and a recent X-ray structural determination of MeCbl furnished an axial Co−N distance of 2.162(4) Å.[5b] On this basis, they define the long distance found by Scheuring et al.[11] as implausible. However, the reason for the appearance of the other minimum in the EXAFS modelling was not clearly established.

In view of the various approaches adopted so far to examine EXAFS data,[8,10−12,20] it is highly desirable to study and discuss the fundamental aspects of EXAFS data analysis of this kind of compound, in order to find a way to standardize analysis of EXAFS results. In fact, despite the fact that it is becoming a common technique, EXAFS may risk losing its credibility among biochemists and chemists because of the above controversy. Therefore, it is essential to better understand what kind of structural information can actually be obtained by EXAFS. We present here an EXAFS methodological study carried out on several cobaloximes, $RCo(DH)_2py$ with R = Cl, N_3, Me, CH_2Ph, adamantyl (adam)[21] (see Figure 1). These cobaloximes were chosen since their structures have been determined with great accuracy.[22] Furthermore, they are stable under measurement conditions and can be handled without the main problems associated with cobalamins, namely their sensitivity to visible light or X-rays.[23] Finally, their axial fragments exhibit as wide a range of bond lengths as possible. These characteristics are essential to carry out an intensive and reliable methodological study. Using B_{12} compounds would have made this work much more complicated, while leaving much room for ambiguity. However, we plan to carry out a similar analysis on B_{12} complexes in the near future. Such a study would have added significance in view of the recent finding that the lengthening due to the trans influence of R in cobalamins is about twice that in cobaloximes.

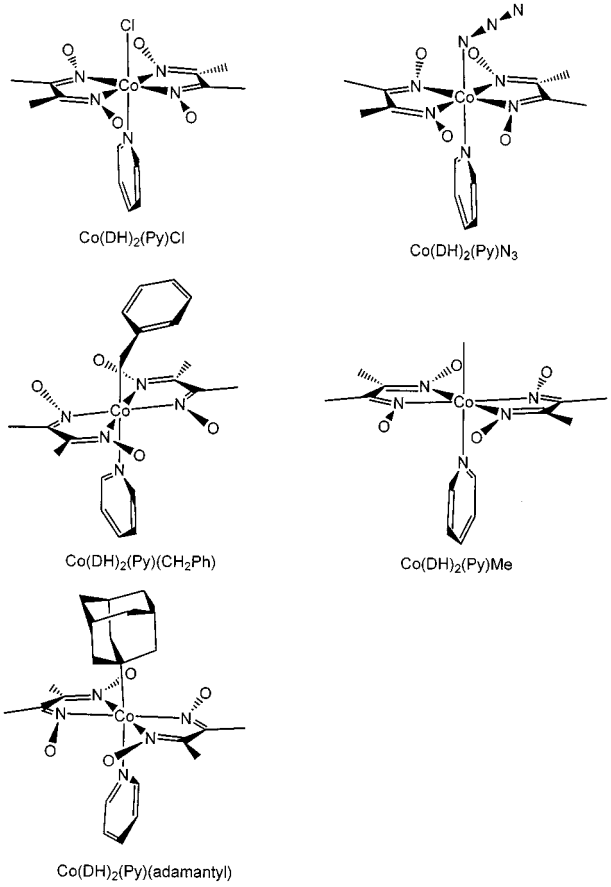

Figure 1. Schemes of the studied complexes, the upper ligand is the only one that changes through the series

Results and Discussion

Limits of the "First-Shell Analysis"

The most common method used to analyze EXAFS data consists of isolating the nearest-neighbours (NN) contributions by Fourier filtering the EXAFS signal. This method has been applied successfully in many cases since the beginning of EXAFS analysis,[24] and its description can be found in a large number of reviews and books.[13,25−27] Although this method is easy to apply because it drastically reduces the complexity of the calculations, it suffers from the limitations discussed in the introduction section. Furthermore, when applying the back-Fourier filtering window, the choice of the limits is not always easy and is always arbitrary. It is a trial and error procedure, while it is often presented as a simple one-way procedure. An example of this and similar problems is given later for R = adam (Figure 2). Finally, if the resolution of EXAFS is expressed as $\Delta r = \pi/(2\Delta k)$, in present case this translates to approximately 0.08−0.10 Å. If the distances do not differ by more than Δr, EXAFS will not resolve them. For the molecules considered in this work, ligands are at distances that differ by approximately 0.1 Å (see Table 2, crystallographic distances) so we are near the limits of the technique.

"First-Shell Analysis" Applied to Cobaloximes

In Table 1, the results of r-space refinements of the first-coordination shell are shown and r-space intervals are shown in Figure 3. When the experimental signal is approximated with a variable number of N atoms at the same distance (Table 1.i), almost 6 neighbours were found only if R = N_3. This should not be surprising: if R = N_3, the Co−R, Co−py, and Co−N(DH)$_2$ distances are quite close (see Table 2, crystal ref.), and this simple model can be used to obtain an acceptable coordination number (CN) and average distance. A lower CN indicates that interference between various contributions reduces the total signal. Therefore, another approach to obtain the actual coordination numbers and distances is to take into account that NN are at two or three different distances. In this case, it has been assumed that 4 N donors are at the same distance (corresponding to the four N donors of (DH)$_2$]. A variable number of N (or Cl or C when indicated in brackets) has been refined as a second contribution to the signal (results are shown in Table 1.ii). In this way, although axial distances are within ±0.05 Å of XRD values (see Table 2, Crystal. ref.), for R = adam, CH_2Ph, and Me, a ligand is apparently missing. For R = Cl, the Cl position is easily determined, but only 4.3 nitrogen atoms are detected in the first shell. Finally, in the case of R = N_3, the coordination number (CN) is correct (5.7 ± 0.4, i.e., 6 NN), but the distance of the first four N donors is 0.05 Å longer, and that of the axial ones is 0.1 Å shorter than the corresponding XRD values. This can be explained in terms of the correlation between the parameters, since the three actual distances are 4 × 1.895, 1 × 1.950, and 1 × 1.973, and it is difficult to resolve them by EXAFS. Finally, a three-distance model, with three free distances and fixed coordination numbers, was employed (the results are reported in Table 1.iii). For R = adam and R = CH_2Ph, the results are acceptable (differences with respect to XRD values are less than ±0.07 Å) and χ^2_v of model ii) and iii) are comparable. On the contrary, for R = Cl, Me, and N_3, errors exceeding 0.1 Å have been found and χ^2_v of model iii) is bigger than that of more

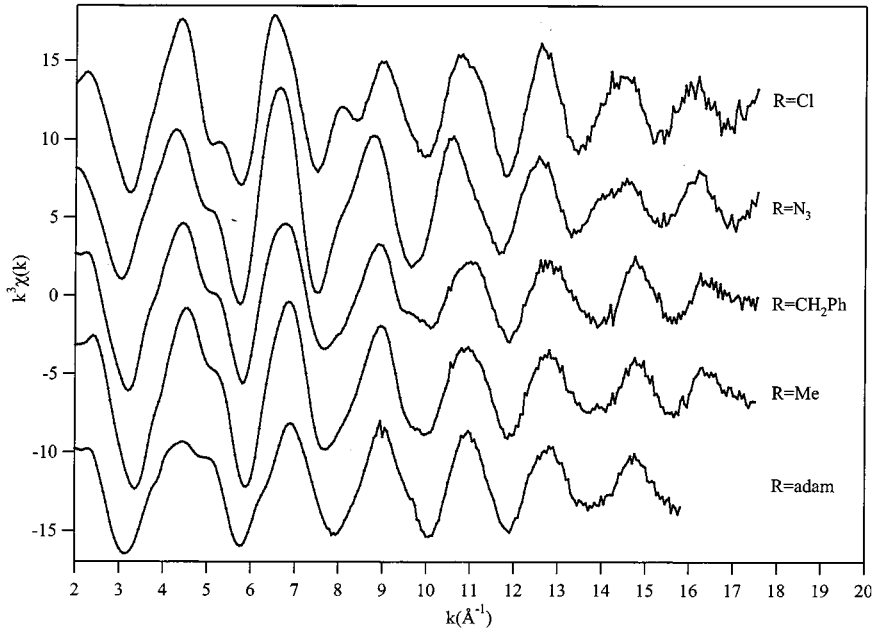

Figure 2. Raw k^3-weighted EXAFS spectra are shown; spectra have been extracted and interpolated on a grid with Δk = 0.02 Å^{-1}; no filtering or smoothing has been applied; spectra are shifted for clarity

Table 1. Results of refinements limited to the first shell; data were obtained with refinements in *r*-space (intervals are shown in Figure 3) assuming i) a model with a variable number of N atoms at the same distance; ii) a model with 4 N at one distance and a variable number of N at another distance (except for R = Cl and Me); iii) a model with 4 N at one distance and the actual atoms of R and Py (N) at a second and third distance, respectively. The refinement degree of freedom is labelled ν

i)	R = adam	R = CH_2Ph	R = Cl	R = Me	R = N_3
N	2.5±0.5	4.0±0.5	/	4.5±0.3	5.6±0.5
σ^2 (Å^2 10^{-3})	2±1	3.8±0.7	/	3.8±0.4	3.7±0.5
R (Å)	1.884±0.009	1.886±0.007	/	1.898±0.004	1.927±0.005
E_0 (eV)	3±3	−4±2	/	3±1	2±2
χ^2_ν	14	3.4		0.93	3
ν	6	3		4	4
ii)	R = adam	R = CH_2Ph	R = Cl	R = Me	R = N_3
N	4	4	4.3±0.6	4	4
σ^2 (Å^2 10^{-3})	3.9±0.5[a]	3.2±0.4[a]	3.3±0.8	3.2±0.3[a]	2±1[a]
R (Å)	1.89±0.01	1.893±0.007	1.918±0.006	1.895±0.006	1.942±0.007
N	1.3±0.5	1.0±0.6	1(Cl)	0.6±0.3(C)	1.7±0.4
σ^2 (Å^2 10^{-3})	3.9±0.5[a]	3.2±0.4[a]	3.2±0.8	3.2±0.3[a]	2±1[a]
R (Å)	2.15±0.03	2.05±0.01	2.247±0.009	2.0±0.04	1.86±0.03
E_0 (eV)	1±4	0±3	3±2	4±2	0±2
χ^2_ν	12.5	2.5	3.9	1.0	3.1
ν	5	2	6	3	3
iii)	R = adam	R = CH_2Ph	R = Cl	R = Me	R = N_3
N	4	4	4	4	4
σ^2 (Å^2 10^{-3})	3.7±0.6[a]	3.4±0.5[a]	2.6±0.8[a]	3.6±0.4[a]	3±1[a]
R (Å)	1.88±0.01	1.89±0.01	1.925±0.007	1.90±0.04	1.94±0.01
N	1	1	1 (Cl)	1	1
σ^2 (Å^2 10^{-3})	3.7±0.6[a]	[a]	3.2±0.7	[a]	[a]
R (Å)	2.12±0.03	2.10±0.03	2.24±0.01	1.9±0.3	1.85±0.05
N	1	1 (C)	1	1 (C)	1
σ^2 (Å^2 10^{-3})	3.7±0.6[a]	[a]	[a]	[a]	[a]
R (Å)	2.23±0.04	2.02±0.05	1.83±0.03	2.07±0.05	1.88±0.07
E_0 (eV)	2±5	1±3	1±2	6±1	0±3
χ^2_ν	15	2.5	4.0	2.0	4
ν	5	2	5	3	3

[a] This symbol indicates that the reported values are the same for a specific model and sample.

simple models. In the case of R = Me the position of Me is undetermined (1.9±0.3 Å). Therefore, unacceptable results are obtained in at least 50% of the cases. The Co−Cl distance and the average distance between cobalt and the four $N(DH)_2$ are accurately determined, because their contributions are dominant.

An Approach to a Complete Simulation

Another way to analyze EXAFS data is to consider the unfiltered spectrum in *k*-space, or an *r*-space interval large enough to cover all relevant peaks (in the studied cobaloximes almost all relevant contributions are below 4 Å). Thus, information from a large number of contributions is included in the analyzed region. On the other hand, the number of independent points is limited (in our case to approximately 25) and is not sufficiently larger than the number of fitted parameters. For this reason, the set of parameters should be carefully chosen before performing a refinement. Care must be taken in choosing the relevant parameters and in linking related quantities, thereby avoiding redundancies. Constraints are based on the knowledge that we have of similar structures. It will be demonstrated that the use of such constraints, whenever possible, is of primary importance. If the system is completely unknown, EXAFS analysis is restricted to a comparison with known systems or first-shell analysis. In most cases, the challenge is to determine which of the several models reproduces the actual structure. In B_{12} model compounds (cobaloximes, in this work) the main problem is to determine the distances of the ligands from cobalt. Schematically a cobaloxime (see Figure 1) may be represented by two coplanar chelate ligands (two DH units referred by a mirror). Thus, the system may be defined by considering ligands as rigid bodies and only specifying the Co−N(DH)$_2$, Co−N(py), and Co−(R) distances and, in the case of R = Ch_2Ph and R = N_3, the angles Co−C_1−C_2 and Co−N_1−N_2 respectively. Actually, such angles are in the range 110°−120° [121.8(1)° for R = N_3[22b] and 116.7(2)° for R = CH_2Ph[22c]]. With regard to the results presented here and in the following discussion, the angles have been fixed at these values. This has been done in order to simplify the calculations and to focus the discussion on the problem of determining distances. However, it has been verified that refinements that include these angles give correct results (within EXAFS accuracy), that is, 127 ± 2° in the case of R = N_3 and 116 ± 3° in the case of R = CH_2Ph. It is worth noting that the use of the structures of rigid bodies directly taken from crystallographic databases suffers from some limitations. Sometimes small

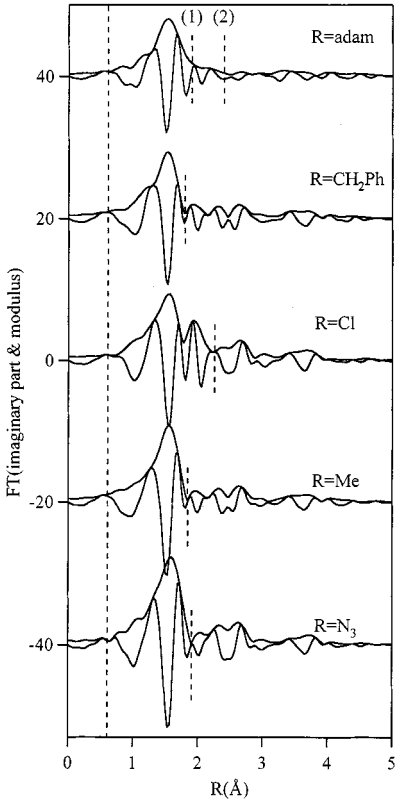

Figure 3. Fourier transform (not phase corrected, imaginary part and modulus plots) of the EXAFS spectra shown in Figure 2; two vertical dashed lines show approximate filtering intervals used to obtain the results in Table 1; for R = adam, two limits (1) and (2) are possible; limit (2) was chosen to obtain the results shown in Table 1; spectra are shifted for clarity

changes (±0.02 Å) to the internal distances can significantly improve the fit of EXAFS data. This happens when two significant contributions interfere, for example, Co−C(DH)$_2$ and Co−O(DH)$_2$ interfere destructively, (see Figures 4 and 5) and their relative distances are critical in determining the signal amplitude. However, it is easy to apply a correction because their contributions are strong and nearly in perfect opposition. Most likely, the best way to do this is a *restrained refinement* as described by Binsted et al.[28] The method used in the present work is a *constrained refinement*,[28] since the former was not possible with the codes in our possession. The remaining relevant parameters are: E_0 to match experiment and theory edge position, S_0^2 (amplitude reduction factor) and a series of Debye−Waller factors (σ_i^2). S_0^2 has been fixed to 1 as suggested by Roy and Gurman[29] (this assumption was tested on $Co(NH_3)_6Cl_3$). The σ_{SS}^2 (single-scattering Debye−Waller factors) values are expected to be very close to each other, and they have been fixed at the same value for similar atoms at similar distances. Only the Co−Cl pair requires its own $\sigma_{Cl,SS}^2$, which is slightly smaller. The MS paths have different σ_i^2, but two relations have been employed to reduce the number of parameters. The σ^2 of triple-scattering paths involving the same couple of atoms in co-linear arrangements is double the single scattering σ_{SS}^2. For example, when the single-scattering (SS) path of Co−N_1−Co has its σ_{SS}^2, the MS path Co−N_1−Co−N_1−Co has $\sigma_{MS}^2 = 2\sigma_{SS}^2$; this was also assumed for paths such as Co−N_1−Co−N_2−Co when N_1 and N_2 are on opposite sides of Co. For triple-scattering paths with angles of approximately 120−160°, instead of using complex relations[20] and due to the homogeneity of the atoms and bonds involved, an average value of three times σ_{SS}^2 has been used. This empirical assumption worked satisfactorily in all five cobaloximes, speeded up calculations while performing contour plots, and did not affect the reliability of the results. Another approach is to calculate Debye−Waller factors using semi-empirical methods.[30] This procedure is flexible and more rigorous, but computationally too heavy for this work. On the other hand, the use of the simple and fast Debye-correlated model is unjustified, even if it was used by other authors for cobalamins.[11] Thanks to the above assumptions the simulation of the entire spectrum required only approximately 6−7 parameters.

Constrained Refinement of Cobaloximes and the Mapping Technique

Numerical results obtained with the assumptions described above are compared with crystallographic distances and listed in Table 2. Distances are determined with some accuracy, but it is evident that discrepancies between XRD and EXAFS are still present. Our EXAFS data were collected at liquid-nitrogen temperature (LNT), while XRD data were collected at room temperature (room temp.). Thus, some small discrepancy is expected, but not as large as 0.05 Å. However, the average accuracy in determining the axial distances with this method can be estimated to be about 0.05 Å. An explanation as to why filtering of the first peak is a risky technique for such molecules can be suggested. The contributions to the EXAFS signal for R = adam (worse simulation) and R = N_3 (better simulation) have been drawn separately in Figure 4 and Figure 5, respectively. In the case of R = adam, the filtering limit used to obtain the results in Table 1 is marked as (2). It is apparent that an important contribution from all NNN (next nearest neighbours) is present well below this limit (see Figure 4). This contribution is not negligible with respect to that of the axial donors. If a narrow filter, as limit (1) in Figure 4, is chosen, almost 50% of the axial contribution is lost (Co−N(Py) and Co−C(adam)]. A different situation is shown in Figure 5 for R = N_3: the first three contributions [Co−N(DH)$_2$, Co−N(Py) and Co−N(N_3)] are in phase and the amplitude of the signal is almost the sum of their amplitudes. This means that the majority of the contributions are included in the filter, and at the same time, the relative importance of the other contributions in the filter is negligible. In fact, for R = N_3, acceptable results have been obtained (see Table 1, a). It is interesting to observe that the Co−C(DH)$_3$ and Co−O(DH)$_2$ contributions (in Figures 4 and 5) have similar amplitudes, and opposite phases giving a very small signal. For this reason, in the region above 2 Å only small features appear, even if several NNN contributions are in that region.

Table 2. Results of fits performed with refinement *c* (see text); crystallographic values are reported for comparison; EXAFS data were recorded at liquid nitrogen temperature, and crystallographic data at room temperature; in the case of R = adam, the crystallographic values are referred to a similar structure where Py is replaced by 4-Me_2N-Py; the refinement degree of freedom is labelled ν

R		Co−N (DH)$_2$		Co−N Py		Co−R		
Adamantyl	EXAFS	1.894	±0.004	2.111	±0.009	2.218	±0.008	Å
	Crystal. ref.	1.876		2.102		2.159		Å
	σ^2_{SS}	3.6	±0.2					10^{-3}Å^2
	χ^2_ν	1.93						
	ν	16						
CH_2Ph	EXAFS	1.887	±0.004	2.07	±0.01	2.00	±0.02	Å
	Crystal. ref.	1.878		2.065		2.056		Å
	σ'^2_{SS}	3.2	±0.3					10^{-3}Å^2
	χ^2_ν	1.26						
	ν	20						
Cl	EXAFS	1.916	±0.005	1.91	±0.02	2.249	±0.004	Å
	Crystal. ref.	1.895		1.959		2.229		Å
	σ^2_{SS}	3.9	±0.2			3.0	±0.3	10^{-3}Å^2
	χ^2_ν	0.79						
	ν	21						
Methyl	EXAFS	1.893	±0.002	2.073	±0.009	1.97	±0.02	Å
	Crystal. ref.	1.896		2.069		1.999		Å
	σ^2_{SS}	3.3	±0.3					10^{-3}Å^2
	χ^2_ν	0.42						
	ν	22						
N_3	EXAFS	1.915	±0.003	1.92	±0.01	1.98	±0.01	Å
	Crystal. ref.	1.895		1.973		1.950		Å
	σ^2_{SS}	3.6	±0.2					10^{-3}Å^2
	χ^2_ν	0.69						
	ν	21						

The finding of multiple solutions, the difference between constrained and unconstrained refinements and the importance of extending the simulation as far as possible should be discussed. For this purpose, χ^2 maps have been calculated. In fact, although constrained refinement dramatically reduces correlation between variables,[28] it does not guarantee that a single solution is found. Some χ^2 maps have been obtained by varying the distances of the axial ligands [Co−N(py), Co−R] and plotting the χ^2, after the other parameters have been refined. Therefore, each point of the grid is the result of an independent refinement. Scattering paths have not been recalculated at each point. Nonetheless, phase and amplitude functions can be regarded as quite accurate in an interval of ±0.2 Å around the contour plot centre. Each minimum of the χ^2 surface is a possible solution to our problem. Contour plots reported in Figures 6, 7, and 8 have been calculated by three different refinement procedures: a) Without constraints; b) With constraints, but limiting the refinement up to 3 Å and thus excluding an isolated large peak between 3 and 4 Å; c) With a constrained refinement up to 4 Å (no contribution is present above 4 Å). Contour plots are presented only for R = adam, CH_2Ph, and Me (Figures 6, 7, and 8, respectively), since they are more representative. Inspection of these plots shows that most contain several minima. For R = adam (Figure 6, a, b, and c), there are always two close minima. They correspond to the interchange of the axial distances (adam at r_1 and py at r_2 or vice versa). The same happens for R = CH_2Ph and Me, as will be discussed later in detail. Looking at Figure 6 (a), two equivalent minima are present. Since C and N are very similar species for EXAFS, swapping the two atoms gives the same solution. If it is important to know at which distance py and adam are, a differentiation between ligands is essential. Constrained refinement is the best tool to differentiate the ligands, but it works only if the interval chosen to make the fit contains significant different contributions from the two ligands. Thus, by refinement b (Figure 6, b) two equivalent minima were found, since the most significant differences between adam and py are above 3 Å. Between 3 and 4 Å, MS is dominant and different geometries can play a significant role. In fact, in plot c, two minima are present, but one is significantly lower than the other. On a statistical basis, it is possible to determine without ambiguity the distance from the metal of each ligand. This means that we can truly distinguish between adam and py. Considering R = CH_2Ph (Figure 7), the maps are more difficult to analyze. At least four minima are present in the centre of map *a*. They can be grouped as follows [Co−C(CH_2Ph); Co−N(py)] ≈ (2.03; 2.08), (2.1; 2.02) and ≈ (1.85; 2.05), (2.05; 1.78). The first two minima correspond approximately to the exchange of the two ligands, as already described for R = adam. The other two

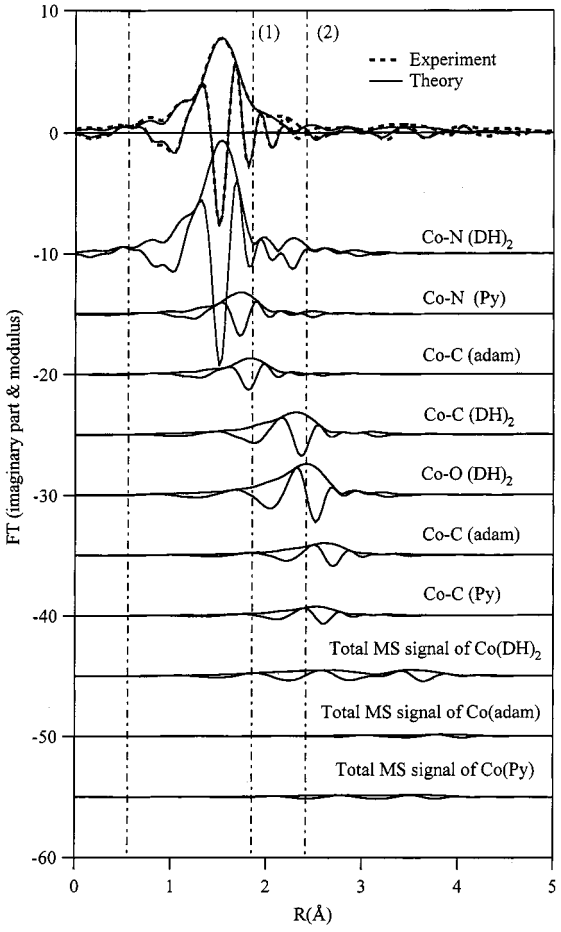

Figure 4. R = adam: comparison of FT (not phase corrected) of experimental and theoretical spectra; all contributions to the total theoretical signal are presented below, ranked for increasing frequency. MS contributions are grouped; spectra are shifted for clarity

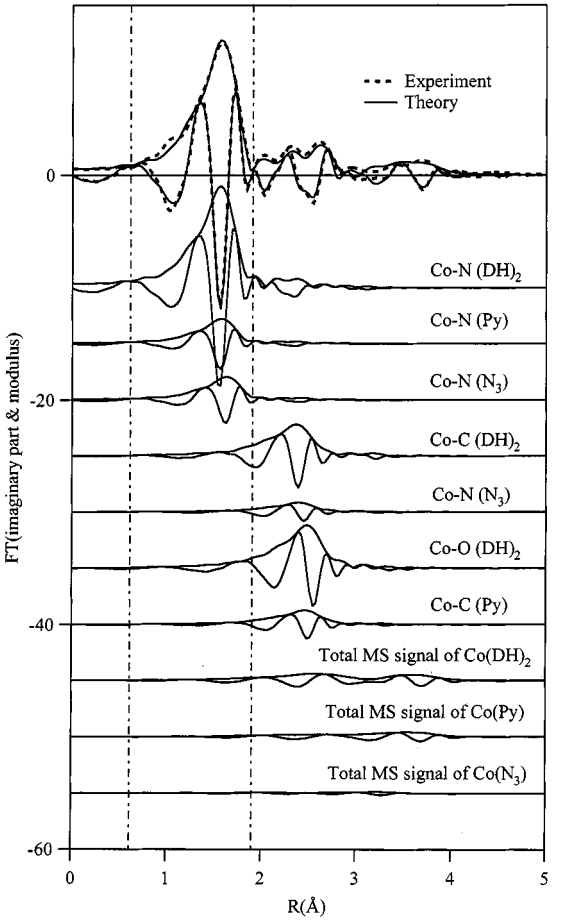

Figure 5. R = N_3: comparison of FT (not phase corrected) of experimental and theoretical spectra; all contributions to the total theoretical signal are presented below, ranked for increasing frequency; MS contributions are grouped; spectra are shifted for clarity

minima correspond to an almost correct position for one of the two axial ligands, while the other is "pushed" into the contribution of the four $N(DH_2)$ donors. Actually, this distance is even shorter than that of $Co-N(DH_2)$. The reasons for the existence of such minima can easily be explained. They are due to the fact that, while fitting the contributions of each atom independently, the $Co-C(CH_2Ph)$ contribution can be masked by the four $Co-N(DH_2)$. A small displacement of the latter and of the Co−N(py) distance then compensates for this error. If the displacement of the atoms in the first shell is linked with that of the bonded atoms and the contributions of the latter are not negligible, this rearrangement is no longer possible. Minima are then better defined, and false minima tend to disappear. For instance, compare plot a with plot b and plot c of Figure 7. Refinement c leads to a marginal improvement, and removes the minimum at $[Co-C(CH_2Ph); Co-N(py)] \approx (1.78; 2.03)$ that can be still obtained by refinement b, but it is possible to discard this solution by the *F*-test. It is worth noting that these "low-distance minima" are also present in Figure 6. These minima are at the lower limits of the map and at a high χ^2 value. In fact, Co−L and Co−R distances for R = adam are longer than for R = CH_2Ph. Thus, they are easier to distinguish and exhibit a poorer correlation with $Co-N(DH_2)$. When R = Me, it is difficult to distinguish py and Me (see minima in Figure 8, a and b) and only with refinement c (when all MS involving the atoms of py are included), can a precise minimum close to XRD results be obtained (see Figure 8, c). Note that in the contour plots for all R (Me, py, CH_2Ph) minima appear at higher distances too. They are always at map upper limits and not perfectly distinguishable, but most likely they correspond to those reported by Champloy et al.[12] The analysis of such far minima is beyond the scope of this paper, since a more complex procedure involving recalculation of scattering paths during refinements should be employed. Work will be carried out in this direction in the future to produce a more flexible and rigorous EXAFS analysis code. However, these far minima appear to be close to the NNN positions. Thus, the explanation is similar to that suggested for the lower distance minima visible in Figure 7 (a).

The approximation of keeping the distance of one axial ligand fixed to an average value obtained from similar structures, while mapping the other, has been reported in

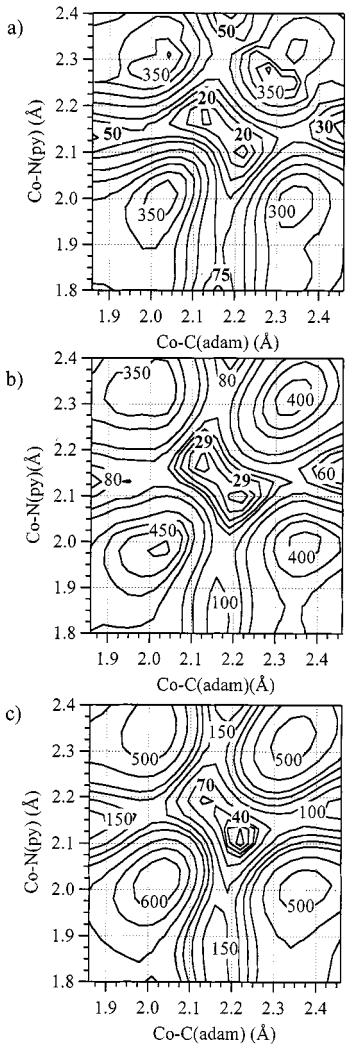

Figure 6. R = adam: contour plots obtained with refinements a, b, and c (see text for details); in case (c) one of the two local minima can be discarded and the axial ligands are distinguishable

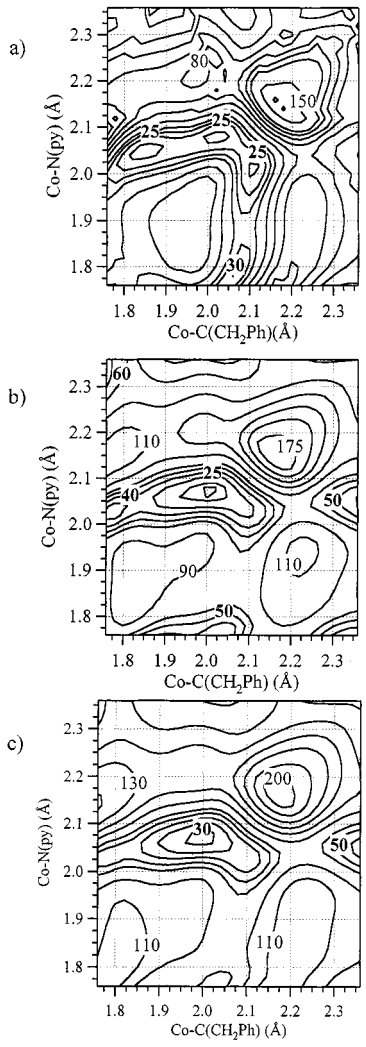

Figure 7. R = CH_2Ph: contour plots obtained with refinements a, b, and c; refinements b and c are almost equivalent (see text for details)

literature.[12] Without questioning the chemical validity of such an assumption, it must be pointed out that in many cases this is risky. In fact, the position of a ligand directly influences the position found for the others. The χ^2 curves obtained by varying the Co−C(Ch_2Ph) distance for different values of the Co−N(py) distance are shown in Figure 9. Co−N(py) values are only 0.02 Å apart, but different χ^2 profiles are obtained. It is apparent that the choice of the "best" minimum for Co−C(Ch_2Ph) distance depends on the value chosen for the Co−N(py) distance (unconstrained refinement).

Finally, with refinement c, answers can be found to such questions as: Is py bonded to Co for R = Cl? Is Me bonded to Co for R = Me? Limiting the analysis to the first shell, the probability of obtaining the presence or absence of the axial ligand (Me, when R = Me; py, when R = Cl) is about 50%. With refinement *c*, the probability that py and Me are bonded (at the correct distance) is at least 75%.

Conclusion

Although the constrained refinement gives an accuracy of about 0.05 Å on the axial distances and an overall correct picture of the actual structure, multiple solutions have been found in some cases. Accordingly to Scheuring et al.,[11] the mapping technique provides a valuable tool to rationalize discrepancies between EXAFS and XRD. It has been shown that multiple minima can be eliminated or discriminated in most cases. The mapping technique plays an essential role in indicating a correct solution and this option should be included in all advanced EXAFS data-analysis codes, together with an advanced constrained/restrained refinement. The principal challenge in fitting EXAFS data of complex systems will be to determine the relevant degrees of freedom of the studied structures and to relate them to as many EXAFS parameters as possible. Thus, the task now is to write codes to integrate ab initio EXAFS calculations,

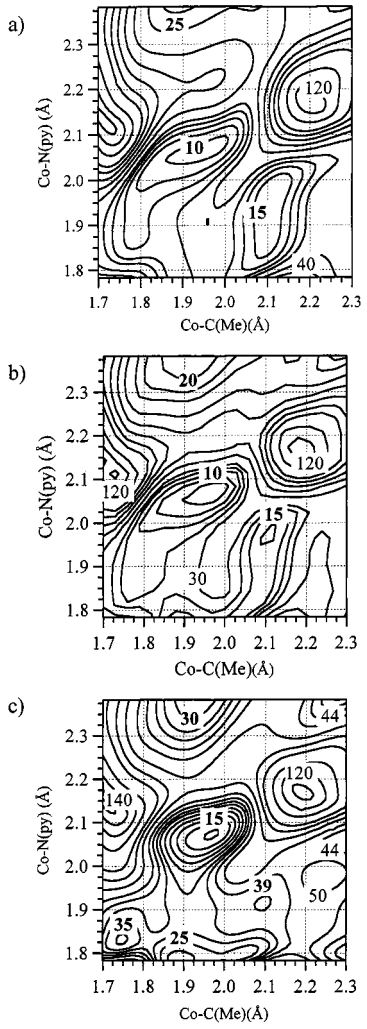

Figure 8. R = Me: contour plots obtained with refinements a, b, and c are shown (see text for details); refinement c is necessary to make the ligands distinguishable

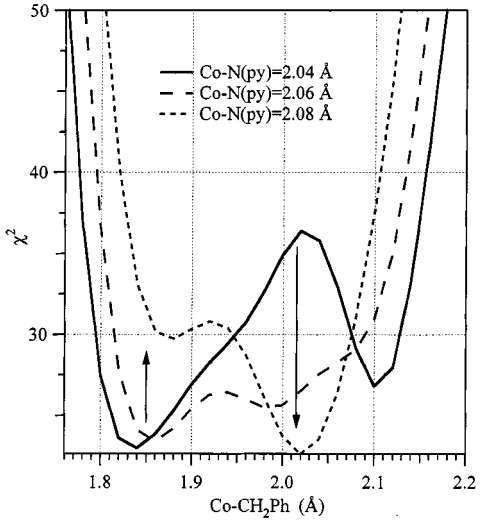

Figure 9. R = CH_2Ph: The χ^2 profile was obtained by varying the Co−CH_2Ph distance for three Co−N(py) values; for very similar values of the latter distance, different values for the Co−CH_2Ph distance were obtained (see position of the minima); arrows indicate minima modifications when the Co−N(py) distance is varied

refinement, and molecular modelling tools, and to make them accessible to the community.

Experimental Section

All reagents and chemicals were commercial products and were used as received. $Co(DH)_2(Py)Cl$,[31] $Co(DH)_2(Py)N_3$,[32] $Co(DH)_2(Py)Me$[32], and $Co(DH)_2(Py)(CH_2Ph)$[33] were synthesized according to reported methods. All these complexes were recrystallized from methanol/H_2O and their purity confirmed by elemental analysis. $Co(DH)_2(Py)$(adamantyl) was obtained by a modification of the synthetic procedure previously reported for the analogous compounds having aniline or 4-dimethylpyridine as axial bases.[22e] Aqueous NaOH solution (2 pellets in 5 mL) was added, with stirring, to dissolve a suspension of $Co(DH)_2(Py)Cl$ (0.8 g, 2 mmol) in methanol (200 mL). While flushing with nitrogen, a suspension of $NaBH_4$ (0.11 g, 3.0 mmol) in water (1 mL) was added, followed by solid 1-iodoadamantane (Aldrich, 1.05 g, 4 mmol). After the solution was vigorously stirred for 40 min, the stream of nitrogen was stopped. The volume of the solution was reduced to ca. 20 mL on a rotary evaporator and the unchanged 1-iodoadamantane was removed by filtration. H_2O (50 mL) was added to the remaining solution, and the red−brown crystals of the desired compound precipitated. The solid was collected by filtration, air dried, and washed with diethyl ether (3 × 10 mL), to remove the residual 1-iodoadamantane. The product was recrystallized by the addition of water to a methanolic solution. Yield 40%. − $C_{23}H_{34}CoN_5O_4$ (503.5): calcd. C 54.9, H 6.81, N 13.9; found C 54.5, H 6.55, N 13.7. − EXAFS data were recorded in the transmission mode at the LURE laboratory (Orsay, France) on beam-line EXAFS-IV in 1999, except for the sample R = adamantyl, which was recorded on EXAFS-1 (now EXAFS-13) in 1994. On beam-line EXAFS-IV, ion chambers were filled with a He/Ne mixture and harmonics were rejected by detuning the two crystals of the Si(331) monochromator. On EXAFS-1, where a Si(331) channel-cut monochromator was the only choice, and no mirrors were available, ion chambers were filled with air to reduce harmonic contamination to a negligible extent. All data were collected at liquid nitrogen temperature. During data analysis, the EXAFS signal $\chi(k)$[34] was multiplied by the cube of the wave-vector modulus $[k^3\chi(k)]$ to balance the decay of the signal due to thermal disorder. Best results were obtained using this weighting, which in some way extends the effective signal range when the signal-to-noise ratio is sufficiently high. Excellent data sets were obtained (see Figure 2). Using a k^0 or k^1 weighting, the signal decayed so quickly that the last part had a small influence on χ^2, and information was partially lost.[16] EXAFS spectra were multiplied by a Hanning window with k_{min} = 3.65 Å^{-1}, k_{max} about 17 Å^{-1} (from 16.5 to 17.5 depending on sample), Δk_{sills} = 2 (except for R = adam: k_{min} = 3.65 Å^{-1}, k_{max} = 14 Å^{-1} Δk_{sills} = 1 Å^{-1}). Fits were performed in *r*-space. We also checked that *k*-space and *r*-space fits did not give results that differed by more than the estimated error bar. Data analysis was carried out on a Red Hat Linux 6.0 powered PC with the UWXAFS suite[35] (Autobk 2.61 and Feffit 2.52 h, version 2.54 for *k*-space fitting) and theoretical standards were obtained using FEFF 7.0.[36] Molecular-modelling structures were obtained from the CSD database, and analyzed with the help of ChemOffice by CambridgeSoft on an iMac. To interface the CSD database and ChemOffice with FEFF 7.0, the Crystalff code was used.[37] The χ^2 maps were obtained using a Perl script to run Feffit on the desired grid points and to archive the results. Contour plots were drawn using Igor Pro 3.0 by WaveMetrics Inc.

Acknowledgments

We thank the Ministero della Ricerca Scientifica e Tecnologica (Roma) (PRIN9803184222) and Consiglio Nazionale delle Ricerche (CNR) for financial support. We are grateful to Dr. K. Provost for code Crystallf, Dr. M. Newville for providing latest improved versions of his Feffit code (2.52 h and 2.54). We acknowledge Dr. F. Champloy for helpful discussions, and the teams of beam-lines EXAFS-13 and EXAFS-IV of LURE for assistance during measurements.

[1] *Vitamin B_{12} and B_{12} Proteins* (Eds.: B. Krautler, D. Arigoni, B. T. Golding); Wiley-VCH, Weinheim, **1998**.
[2] *Chemistry and Biochemistry of vit B12* (Ed.: R. Banerjee),, J. Wiley & sons, N.Y. **1999**
[3] [3a] N. Bresciani-Pahor, M. Forcolin, L. G. Marzilli, L. Randaccio, M. F. Summers, J. P. Toscano, *Coord. Chem. Rev.* **1985**, *63*, 1. – [3b] B. T. Golding, *J. R. Neth. Chem. Soc.* **1987**, *106*, 342. – [3c] L. Randaccio, N. Bresciani-Pahor, E. Zangrando, L. G. Marzilli, *Chem. Soc. Rev.* **1989**, *18*, 225. – [3d] L. Randaccio, *Comm. Inorg. Chem.* **1999**, *21*, 327.
[4] L. Randaccio, S. Geremia, M. Furlan, M. Slouf, *Inorg. Chem.* **1998**, *37*, 5390.
[5] [5a] L. Randaccio, S. Geremia, G. Nardin, M. Slouf, I. Srnova, *Inorg. Chem.* **1999**, *38*, 4087. – [5b] L. Randaccio, M. Furlan, S. Geremia, M. Slouf, I. Srnova, D. Toffoli, *Inorg. Chem.* **2000**, in press.
[6] C. Kratky, G. Färber, K. Gruber, Z. Deuter, H. F. Nolting, R. Konrat, B. Kräutler, *J. Am. Chem. Soc.* **1995**, *117*, 4654.
[7] [7a] I. Sagi, M. D. Wirt, E. Chen, S.M. Frisbie, M. R. Chance, *J. Am. Chem. Soc.* **1990**, *112*, 8639. – [7b] M. D. Wirt, I. Sagi, E. Chen, S. M. Frisbie, R. Lee, M. R. Chance, *J. Am. Chem. Soc.* **1991**, *113*, 5299.
[8] I. Sagi, M. R. Chance, *J. Am. Chem. Soc.* **1992**, *114*, 8061 (cyano and aquo).
[9] E. M. Scheuring, I. Sagi, M. R. Chance, *Biochemistry* **1994**, *33*, 6310 (Co−S).
[10] M. Giorgetti, M. Berrettoni, P. Conti, R. Di Cicco, R. Marassi, I. Ascone, *Organometallics* **1996**, *15*, 3491.
[11] E. Scheuring, R. Padmakumar, R. Banerjee, M. R. Chance, *J. Am. Chem. Soc.* **1997**, *119*, 12192.
[12] F. Champloy, G. Jogl, R. Reitzer, W. Buckel, H. Bothe, B. Beatrix, G. Broeker, A. Michalowicz, W. Meyer-Klaucke, C. Kratky, *J. Am. Chem. Soc.* **1999**, *121*, 11780.
[13] H. Bertagnolli, T. S. Hertel, *Angew. Chem. Int. Ed. Engl.* **1994**, *33*, 45.
[14] P.F. Lidley, in: *X-ray Absorption Fine Structure* (Ed.: S. S. Hasnain), Ellis Horwoord Ldt, Chichester, England, **1999**, 115.
[15] P. A. Lee, H. Citrin, P. Eisenberger, B. M. Kincaid, *Rev. Mod. Phys.* **1981**, *53*, 769
[16] A. Michalowicz, K. Provost, S. Laruelle, A. Mimouni, G. Vlaic, *J. Synchrotron Rad.* **1999**, *6*, 233 (XAFS-X conference proceeding, Chicago)
[17] A. Mimouni, Thesis, University of Paris XII, France, **1997**.
[18] L. Randaccio, S. Geremia, *Organometallics* **1997**, *16*, 4951.
[19] F. Mancia, N. H. Keep, A. Nakagawa, P. F. Leadlay, S. McSweeney, B. Rasmusssen, P. Boesecke, O. Diat, P. R. Evans, *Structure* **1996**, *4*, 339.
[20] Tami E. Westre, A. Di Cicco, A. Filipponi, C. R. Natoli, B. Hedman, E. I. Solomon, K. O. Hodgson, *J. Am. Chem. Soc.* **1995**, *117*, 1566.
[21] In the case of R = adam, the neutral ligand is 4-Me_2N-py.
[22] [22a] S. Geremia, R. Dreos, L. Randaccio, G. Tauzher, L. Antolini, *Inorg. Chim. Acta* **1994**, *216*, 125. – [22b] M. N. Ponnuswamy, J. Trotter, *Acta Crystallogr., Sect. C (Cr. Str. Comm.)* **1983**, *39*, 726. – [22c] N. Bresciani Pahor, L. Randaccio, E. Zangrando, L. Antolini, *Acta Crystallogr., Sect. C(Cr. Str. Comm.)* **1988**, *44*, 2052. – [22d] A. Bigotto, E. Zangrando, L. Randaccio, *J. Chem Soc., Dalton Trans.* **1976**, 96. – [22e] N. Bresciani Pahor, L. Randaccio, E. Zangrando, P. A. Marzilli, *J. Chem. Soc., Dalton Trans.* **1989**, 1941.
[23] F. Champloy, K. Gruber, G. Jodl, C. Kratky, *J. Synchrotron Rad.* **2000**, *7*, 267.
[24] D. E. Sayers, E. A. Stern, F. W. Lytle, *Phys. Rev. Lett.* **1971**, *27*, 1204.
[25] P. A. Lee, H. Citrin, P. Eisenberger, B. M. Kincaid, *Rev. Mod. Phys.* **1981**, *53*, 769
[26] *EXAFS: Basic principles and Data Analysis* (Ed.: Boon K. Teo), Springer Verlag, Berlin, **1986**.
[27] *X-ray Absorption Fine Structure* (Ed.: S. S. Hasnain), Ellis Horwood-Publishers, New York, **1991.**
[28] N. Binsted, R. W. Strange, S. S. Hasnain, *Biochemistry* **1992**, *31*, 12117.
[29] M. Roy, S. J. Gurman, *J. Synchrotron Rad.* **1999**, *6*, 228.
[30] M. Benfatto, C. R. Natoli, A. Filipponi, *Physical Review B* **1989**, *40*, 9626.
[31] N. Dimakis, M.-Ali Al Akhras, G. Bunker, *J. Synchrotron Rad.* **1999**, *6*, 266.
[32] G. N. Schrauzer, *Inorganic Syntheses* **1968**, *11*, 61.
[33] A. Clearfield, R. Gopal, R. J. Kline, M. L. Sipski, L. O. Urban, *J. Coord. Chem.* **1978**, *8*, 5.
[34] G. N. Schrauzer, E. Deutsch, *J. Am. Chem. Soc.* **1970**, *91*, 3341.
[35] The notation could be confusing: $\chi(k)$ is the EXAFS signal, while χ^2 and χ^2_ν are statistical functions.
[36] E. A. Stern, M. Newville, B. Ravel, Y. Yacoby, D. Haskel, *Physica B* **1995**, *208−209*, 117.
[37] J. J. Rehr, C. H. Booth, F. Bridges, S. I. Zabinsky, *Phys. Rev. B* **1994**, *49*, 12347
[38] K. Provost, A. Michalowicz, *J. Synchrotron Rad.* **2000**, manuscript submitted.

Received August 16, 2000
[I00316]